MIT Open Access Articles

Identification of Novel Fibrosis Modifiers by In Vivo siRNA Silencing

Identification of Novel Fibrosis Modifiers
by In Vivo siRNA Silencing

Elisabeth H. Vollmann,[1] Lizhi Cao,[1] Aldo Amatucci,[1,7] Taylor Reynolds,[1] Stefan Hamann,[1] Isin Dalkilic-Liddle,[1]
Thomas O. Cameron,[1] Markus Hossbach,[2] Kevin J. Kauffman,[3] Faryal F. Mir,[3] Daniel G. Anderson,[3]
Tatiana Novobrantseva,[4] Victor Koteliansky,[5] Tatiana Kisseleva,[6] David Brenner,[6] Jeremy Duffield,[1]
and Linda C. Burkly[1]

[1]Biogen, Inc., Cambridge, MA 02142, USA; [2]Axolabs, GmbH, 95326 Kulmbach, Germany; [3]David H. Koch Institute for Integrative Cancer Research, MIT, Cambridge, MA
02139, USA; [4]Verseau Therapeutics, Auburndale, MA 02466, USA; [5]Skolkovo Institute of Science and Technology, Moscow 143026, Russia; [6]Department of Medicine,
University of California, San Diego, San Diego, CA 92093, USA

Fibrotic diseases contribute to 45% of deaths in the industrialized world, and therefore a better understanding of the pathophysiological mechanisms underlying tissue fibrosis is sorely needed. We aimed to identify novel modifiers of tissue fibrosis expressed by myofibroblasts and their progenitors in their disease microenvironment through RNA silencing in vivo. We leveraged novel biology, targeting genes upregulated during liver and kidney fibrosis in this cell lineage, and employed small interfering RNA (siRNA)-formulated lipid nanoparticles technology to silence these genes in carbon-tetrachloride-induced liver fibrosis in mice. We identified five genes, *Egr2, Atp1a2, Fkbp10, Fstl1,* and *Has2,* which modified fibrogenesis based on their silencing, resulting in reduced *Col1a1* mRNA levels and collagen accumulation in the liver. These genes fell into different groups based on the effects of their silencing on a transcriptional mini-array and histological outcomes. Silencing of *Egr2* had the broadest effects in vivo and also reduced fibrogenic gene expression in a human fibroblast cell line. Prior to our study, *Egr2, Atp1a2,* and *Fkbp10* had not been functionally validated in fibrosis in vivo. Thus, our results provide a major advance over the existing knowledge of fibrogenic pathways. Our study is the first example of a targeted siRNA assay to identify novel fibrosis modifiers in vivo.

INTRODUCTION

Pathological tissue fibrosis is the abnormal accumulation of collagen-rich extracellular matrix (ECM) after a chronic or misregulated response to injury that progressively disrupts tissue architecture, leading to tissue stiffness, impaired organ function, and eventually organ failure. Fibrosis is featured in diverse conditions, accounts for as much as 45% of all deaths worldwide, and appears to be increasing in prevalence.[1] Fibrosis complications arise in very different disease settings, from autoimmunity and environmentally induced inflammation to cancer, spanning multiple organs. To date, the treatment options are extremely limited for attenuating or reversing this process. Thus, there is an urgent need to delineate underlying pathological mechanisms that may lead to new therapeutic approaches.

Both the initiation and persistence of pathological fibrosis involves the activation and differentiation of progenitors to myofibroblasts, the key effectors in fibrosis.[2] Myofibroblasts play an important role in executing physiologic tissue repair, leading to matrix deposition, wound contraction, and healing on one hand, and pathological fibrogenesis leading to chronic fibrosing conditions on the other.[3] Accordingly, prominent molecular pathways in acute tissue repair often recapitulate their fibrogenic function in chronic fibrotic conditions, essentially conditions in which wound healing has gone awry; these include platelet derived growth factor receptor beta (PDGFRβ) and transforming growth factor beta (TGF-β). However, there are still many gaps in our understanding of the mechanisms underlying fibrogenesis. Due to their morphology and function, these cells are incredibly difficult to study in vitro. Recently, elegant fate mapping studies pointed to a role for pericytes as a significant progenitor pool for myofibroblasts after injury in a variety of organ systems.[4] Liver pericytes, also known as hepatic stellate cells (HSCs), have been shown to be the major progenitor pool for myofibroblasts after carbon tetrachloride (CCl4)-induced liver injury and fibrosis,[5,6] and gene expression profiling of these cells isolated at various time points after CCl4 administration identified molecular alterations that might be functionally relevant to fibrogenesis.[6] Likewise, myofibroblasts and their precursors have been transcriptionally profiled during kidney fibrosis in mice using translational ribosome affinity purification technology.[7] Isolation of this cell type induces a lot of alteration in what these cells express; therefore, it is important to study the function of the genes in their native disease environment without disrupting cell-cell and cell-matrix interactions.

We aimed to identify novel modifiers of tissue fibrosis expressed in myofibroblasts or their progenitors through RNA silencing in vivo.

CrossMark

Although much more challenging than conducting a cell-based screen in vitro, this in vivo approach was pursued to enable the interrogation of gene function in the context of the complex tissue environment and thereby yield physiologically relevant fibrosis modifiers. In order to achieve this objective, we employed recently generated transcriptomes from myofibroblasts and their precursors in models of liver and kidney injury and fibrosis.[6,7] To achieve effective gene silencing in vivo, we used small interfering RNA (siRNA) delivery with lipid nanoparticles (siRNA-LNPs), an emerging technology for gene silencing in vivo, particularly in the liver,[8] and hence deployed this technology in a model of liver fibrogenesis. The siRNA-LNP technology has been previously used to show that silencing of the collagen type I alpha 1 gene (*Col1a1*) reduced its mRNA levels and collagen accumulation in liver fibrosis models.[9,10] However, the use of siRNA-LNP technology in a targeted assay for identifying novel fibrosis modifiers has not yet been reported. Herein, we report our use of a platform composed of novel siRNA targets, siRNA-LNP delivery technology, and CCl$_4$-induced liver fibrosis, resulting in the identification of novel modifiers of fibrogenesis in vivo.

RESULTS

Targeted Genomic Screening Strategy

We aimed to silence genes in key fibrogenic cell lineages, myofibroblasts, and pericytes to identify novel mediators of tissue fibrosis. Candidate genes were selected by the intersection of gene expression datasets for this cell lineage in two different organ systems. We identified genes that were commonly at least 2-fold upregulated in activated HSCs isolated from livers of mice treated with CCl$_4$ for 2 months[6] and myofibroblasts and pericytes, their precursors, in the mouse kidney 2 and 5 days after unilateral ureteral obstruction (UUO).[7] 169 genes met this criterion. We excluded transcripts that were not associated with a gene product, had no human homolog, or had well-known functions in fibrosis (Figure 1). Ultimately, we unbiasedly tested 24 genes by siRNA-mediated gene knockdown (KD) in vivo (Table S1).

Establishment of CCl$_4$-Induced Liver Fibrosis and Validation of the siRNA KD Approach in Mice

CCl$_4$-induced liver injury and fibrosis in mice is a well-characterized model consisting of repeated CCl$_4$ administration that injures hepatocytes, followed by a fibrogenic reaction. HSCs are activated to expand, differentiate to myofibroblasts, and produce increased levels of ECM and pro-inflammatory mediators, thereby also promoting macrophage accumulation; all of these reactions constitute a coordinated response to tissue injury and the progressive accumulation of collagen. We found that animals dosed orally with 1 mL/kg of CCl$_4$ in mineral oil on day 0 and day 7 and euthanized on day 10 exhibited significant liver fibrosis based on increased picrosirius red (PSR) and collagen immunopositivity in liver tissue as compared to vehicle-treated mice. Percent area of tissue immunoreactive with aSMA, the hallmark of myofibroblasts, and IBA-1, a macrophage-specific marker, were also increased in CCl$_4$-treated animals, suggesting an increase in myofibroblasts and macrophage numbers in the tissue (Figures S1A–S1C). Corresponding to increased collagen deposition in
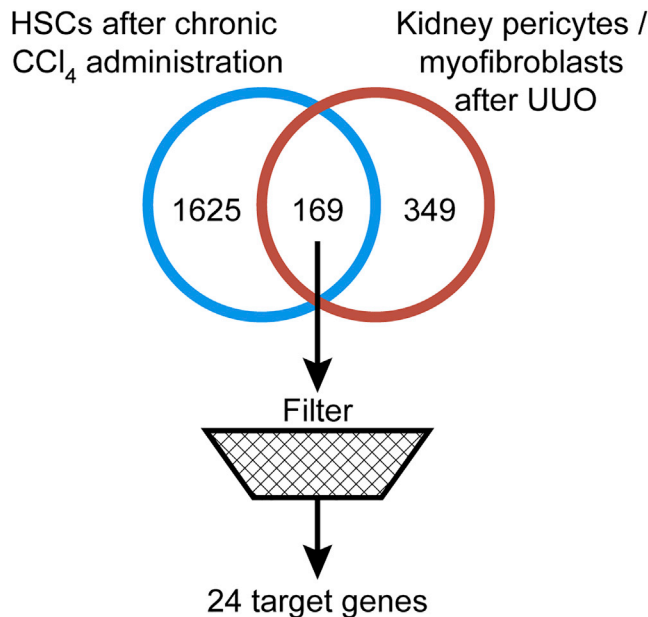

Figure 1. Targeted Genomic Screening Strategy
Intersection of differentially expressed genes upregulated in hepatic stellate cells after chronic CCl$_4$-induced liver injury and genes specific to renal pericyte/myofibroblast lineage after unilateral ureteral obstructions in mice. 169 commonly upregulated genes were subjected to a filter to exclude those with a well-known role in fibrosis or with no human homolog or with unknown product, yielding 24 target genes of interest.

tissue, *Col1a1* mRNA was markedly upregulated (Figure S2A). The assessment of *Col1a1* mRNA levels was used as an expedient approach to functionally assess a relatively large number of siRNA targets and flag fibrogenic genes of interest.

Given the siRNA-LNP delivery system targets multiple liver cell types, including HSCs, hepatocytes, Kupffer cells, but not endothelial cells,[11–14] we validated the ability to KD genes expressed in HSCs in mice using siRNA-LNPs (Figures S1D–S1H). Mice were injected with a single dose of siRNA-LNP (1 mg/kg) against *Reelin* (*Reln*-LNPs), a gene prominently expressed in HSCs.[15] Animals receiving *Reln*-LNPs, but not *Luc*-LNPs (negative control), showed significant reduction in *Reln* mRNA in both oil- and CCl$_4$-treated animals (Figure S1E). We also demonstrate the ability to KD the HSC-specific gene *Col1a1* in liver. *Col1a1*-LNP reduced *Col1a1* mRNA by 50%, with no effect on *Reln* mRNA. Because the TGF-β pathway is a recognized fibrogenic mediator, we tested whether KD of transforming growth factor beta receptor 1 (*Tgfbr1*) decreased the transcription and accumulation of collagen. Indeed, administration of *Tgfbr1*-LNPs and *Col1a1*-LNPs, but not *Luc*-LNPs, reduced the transcription of *Col1a1* mRNA (Figure S1F) as well as collagen accumulation (Figures S1G and S1H).

To test the role of genes identified in our transcriptomic analysis, we modified the siRNA administration protocol to allow pre-existing
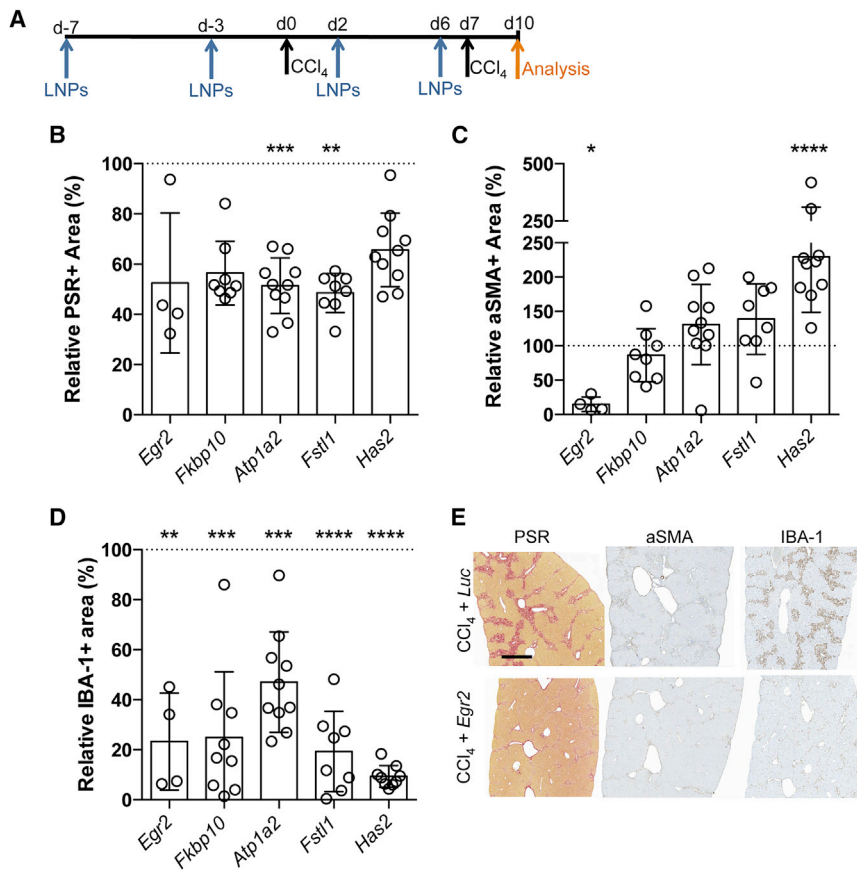
Figure 2. Analysis of Fibrosis Modifiers

(A) Schematic of the experimental design showing animals dosed with CCl_4 on day 0 and day 7, siRNA-LNPs administered on day −7, −3, 2, and 6, and liver tissue analyzed on day 10. (B–D) Graphs show the effect of siRNA-KD of the indicated genes (x axis) on the accumulation of collagen (% PSR positive area/total tissue area) (B), % aSMA immunopositive area/total tissue area (C), and % IBA-1 positive area/total tissue area (D) relative to that obtained with *Luc*-LNPs administered in CCl_4-treated mice in the same experiment. Each symbol represents an individual animal. Data are displayed as mean ± SD. Statistically significant differences were evaluated using one-way ANOVA and Dunnett's post test. Adjusted P values of less than 0.05 were considered statistically significant with *$p < 0.05$; **$p < 0.01$; ***$p < 0.001$; and ****$p < 0.0001$. (E) Representative micrographs of PSR (left panel), aSMA (middle panel), and IBA-1 (right panel) immunoreacted liver section of CCl_4/*Luc*-LNP (upper row) or CCl_4/*Egr2*-LNP (lower row) treated animals. Scale bar, 1 mm.

levels. Silencing of these genes did not elicit any overt toxicity, as measured by body weight loss (Figure S3). Because the other 19 genes did not meet these criteria (Tables 1 and S1), we focused on further analyzing the five modifiers of fibrosis.

The KD of the transcription factor (TF) *Egr2* had the broadest effect by reducing the levels of *Col1a1* and *Col3a1* mRNA as well as the percent area immunopositive for aSMA, IBA-1, and collagen proteins, although the reduction in collagen by half did not achieve significance (Figure 2; Table 1). *Egr2* silencing also reduced *Pdgfrb* mRNA levels (Figure 3A), suggesting a mechanism of decreased fibrosis and macrophage accumulation due to reduced expansion of activated HSCs. Given that *Egr2* has structural similarities to its family members, *Egr1* and *Egr3*, we confirmed the specificity of the *Egr2* siRNA by transfecting human 293T cells with plasmids encoding mouse *Egr1*, *Egr2*, or *Egr3* under the transcriptional control of the CMV promoter. In the tested construct, the expression of mouse *Egr1*, *Egr2*, and *Egr3* is not under the control of the endogenous promoter. Thus, reduction in gene expression is due to the binding of the siRNA *Egr2* to the mRNA. Using the same *Egr2* siRNA that was used for the in vivo experiments, we found that this siRNA reduced *Egr2* mRNA levels, but not *Egr1* or *Egr3* mRNA, unambiguously demonstrating that *Egr1* and *Egr3* were not targeted by our *Egr2* siRNA (Figures S4A–S4C). Interestingly, even though the siRNA against *Egr2* was specific, *Egr2*-LNP treatment in vivo also reduced *Egr1* and *Egr3* mRNA levels (Figures S4D–S4F), suggesting transcriptional co-regulation of EGR family members.

Similar to *Egr2*, KD of *Fkbp10* or *Atp1a2* reduced the collagen and IBA-1 positive areas as did that of *Egr2* (Figure 2; Table 1); however,

protein to be turned over and therefore achieve pre-clearance of proteins encoded by the genes of interest and ensure continued KD throughout the experiment (Figure 2A). We first used *Luc*-LNPs to validate this protocol for detecting differences between oil- and CCl_4-treated cohorts, with respect to the levels of *Col1a1* mRNA, our primary parameter for defining target genes. We similarly evaluated differences in the mRNA levels for a panel of other genes (Figure S2A). The strictly standardized mean difference (SSMD) values for *Col1a1*, collagen type III alpha 1 (*Col3a1*), tissue inhibitor of metalloproteinases 1 (*Timp1*), and platelet derived growth factor receptor beta (*Pdgfrb*), but not *Tgfbr1*, integrin subunit alpha M (*Itgam*), or alpha-actin-2 (*Acta2*), suggested that these genes were suitable to use as readout genes (Figure S2B).

Identification of Fibrosis Modifiers

Having established the suitability of the CCl_4 treatment with the siRNA-LNP KD platform, we proceeded to test our candidate genes. We tested the effect of KD of 24 individual genes in vivo (Figure 2A). We identified seven genes that significantly reduced the amount of *Col1a1* mRNA (Table 1). Five of these seven genes, namely, early growth response 2 (*Egr2*), FK506-binding protein (*Fkbp10*), ATPase Na⁺/K⁺ transporting subunit alpha 2 (*Atp1a2*), follistatin like 1 (*Fstl1*), and hyaluronan synthase 2 (*Has2*), were silenced by 75%–100% in whole liver tissue and significantly reduced *Col1a1* mRNA

Table 1. Fibrosis Modifiers in CCl₄-Induced Liver Fibrosis Identified by siRNA KD

Target	KD (%)	Relative *Col1a1* mRNA (%)	Relative *Col3a1* mRNA (%)	No. of Other Readout Genes Up	No. of Other Readout Genes Down	Relative Positive PSR Area (%)	PSR Non-adjusted p Value	Relative aSMA-Positive Area (%)	aSMA Non-adjusted p Value	Relative IBA-1-Positive Area (%)	IBA-1 Non-adjusted p Value
Egr2	94.1	15.1*	46.7**		1[a]	54.5	0.0145	14.8*	0.0034	15.4**	0.0241
Fkbp10	74.7	25.1****	76.1		1[a]	64.4	0.0150	79.4	0.3322	16.5***	0.0036
Atp1a2	97.8	62.1**	99.9		1[b]	51.4***	<0.0001	130.9	0.1167	47.1****	<0.0001
Fstl1	78.6	39.3**	96.9	1[b]		48.5**	0.0009	179.7	0.0800	12.7****	0.0034
Has2	100	29.1****	97.3	1[b]		65.6	0.0155	229.5****	<0.0001	8.1****	0.0011
Dpysl3	46.7	40.7**	96.1		1[b]	100.3	0.9850	20.3	0.0628	26.1***	0.0122
Crlf1	24.8	54.7*	86.5		2[a,c]	101.1	0.9998	68.5	0.3232	118.6*	0.0053

The gene-specific KD of the indicated gene itself as well as the relative gene expression of *Col1a1* and *Col3a1* compared to *Luc*-LNP-treated animals were tabulated. Statistically significant differences were evaluated using one-way ANOVA and Dunnett's post test. Adjusted p values < 0.05 were considered statistically significant, with *p < 0.05; **p < 0.01; ***p < 0.001; and ****p < 0.0001. Non-adjusted p values are also tabulated. *Dpysl3*, dihydropyrimidinase like 3; *Crlf1*, cytokine receptor like factor 1.
[a]*Pdgfrb*.
[b]*Timp1*.
[c]*Tgfbr1*.

KD of *Fkbp10* or *Atp1a2* did not alter the percent immunopositivity for aSMA. *Fkbp10* KD also decreased *Pdgfrb* mRNA levels, but this effect was somewhat weaker than that of *Egr2* (28% versus 45% reduction; Figures 3A and 3B), possibly accounting for its lack of effect on aSMA immunopositivity. *Atp1a2* KD also decreased *Timp1* mRNA levels (Figure 3C). These results suggest that *Egr2*, *Fkbp10*, and *Atp1a2* regulate fibrogenesis through different mechanisms.

KD of either of the two other fibrosis modifiers, *Fstl1* and *Has2*, decreased *Col1a1* mRNA levels as well as macrophage and collagen accumulation in the tissue, although *Has2* KD did not achieve significance for the latter (Figure 2). Notably, KD of these genes showed increased amounts of aSMA immunopositivity, which was highly significant for *Has2* KD, suggesting increased numbers of myofibroblasts. Corresponding with the increased myofibroblasts, we detected higher levels of the *Timp1* mRNA in the livers of both *Fstl1* and *Has2* KD animals (Figures 3D and 3E). Despite the increased myofibroblast and *Timp1* mRNA levels, *Fstl1* KD significantly reduced collagen accumulation. In order to understand these findings, we also conducted in parallel in vitro studies and showed that three independent *FSTL1* siRNAs reduced *COL1A1* mRNA levels. Thus, the direct reduction of collagen transcription may be sufficient to reduce overall collagen accumulation, despite the elevated number of myofibroblasts and reduced collagen degradation (Figure S5).

Silencing of *EGR2* in Human HSCs Reduces Expression of Fibrogenic Genes

EGR2 emerged as the strongest modifier of fibrosis in the CCl₄ liver fibrosis/siRNA KD platform. We aimed to directly demonstrate that *EGR2* KD in an HSC would reduce *COL1A1* and *PDGFRB* mRNA levels. We tested the effect of *EGR2* KD in the human HSC line LX-2 using three independent siRNAs (Figure 4). This experiment required a different siRNA to be used because no species cross-reactive siRNA was designed (see Materials and Methods). All siRNAs against *ERG2* reduced its mRNA levels as well as *COL1A1* and *PDGFRB* mRNA levels. These results are consistent with the effect of *Egr2* KD in our in vivo CCl₄ assay platform. As expected, KD of *COL1A1* reduced its own expression, but not that of *EGR2*. Interestingly, *COL1A1* silencing also reduced *PDGFRB* mRNA levels, suggesting a regulatory feedback loop. Taken together, these data support that EGR2 is fibrogenic in both rodents and humans.

DISCUSSION

There are currently limitations in the understanding of pathophysiological mechanisms underlying fibrotic diseases. Myofibroblasts are key effectors of fibrosis and therefore the elucidation of pathways that promote this cell lineage would be a significant advance in the field. Here, we report the use of a targeted in vivo siRNA KD platform to identify novel mediators of fibrogenesis. We leveraged novel biology-targeting genes upregulated during liver and kidney fibrosis in myofibroblasts and their progenitors and siRNA-LNP technology to silence these genes in CCl₄-induced liver injury and fibrosis in mice. We identified five genes, namely *Egr2*, *Atp1a2*, *Fkbp10*, *Fstl1*, and *Has2*, which modified fibrogenesis in this system because their KD reduced *Col1a1* mRNA levels and collagen accumulation in the liver. Prior to our study, *Egr2*, *Atp1a2*, and *Fkbp10* had not been functionally validated in fibrosis in vivo, and our study is the first to validate *Fstl1* and *Has2* in liver fibrosis. We further directly demonstrated that *Egr2* KD in human HSCs reduced the expression of fibrotic genes. We conclude that in vivo siRNA KD using siRNA-LNP is a powerful tool to identify disease-relevant modifiers in vivo.

Studying myofibroblasts is extremely difficult because they are in direct contact with multiple cell types, including other myofibroblasts, myeloid cells, mesothelial cells, endothelial cells, epithelial cells, and
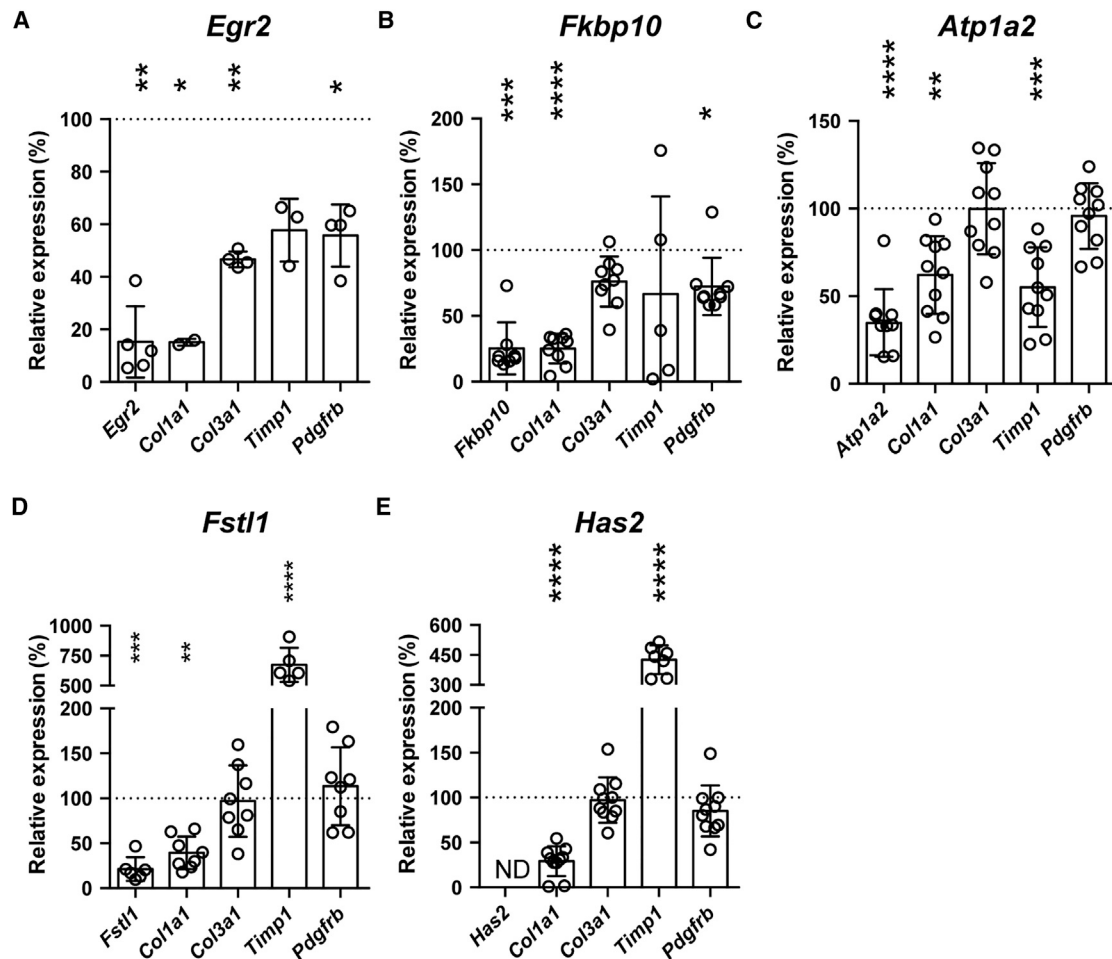
Figure 3. Effect of Gene Silencing on mRNA Levels of a Panel of Readout Genes

(A–E) qPCR data of indicated readout genes (x axis) of animals that have received siRNA-LNPs targeting *Egr2* (A), *Fkbp10* (B), *Atp1a2* (C), *Fstl1* (D), or *Has2* (E) were plotted as percentage of *Luc*-LNP treated animals within the same experiment. n = 4–15 animals per group. Data are presented as mean ± SD. Statistical comparisons were performed using one-way ANOVA and Dunnett's post test. Statistical differences are indicated as *$p < 0.05$; **$p < 0.01$; ***$p < 0.001$; and ****$p < 0.0001$. ND, not detected.

circulating fibrocytes in situ.[16] Myofibroblasts respond to chemo-mechanical stimuli, and therefore disruption of their native environment during cell isolations alters their activation state. To circumvent these shortcomings, we silenced target genes in vivo by systemic administrating siRNA-LNPs. This approach allowed us to study functional consequences of silencing of specific genes of interest in vivo in their native environment. It is of note that our siRNA-LNP delivery approach allows us to silence gene expression in HSCs; however, this LNP formulation also targets other cells in the liver, including Kupffer cells and hepatocytes, but not endothelial cells.[11–14] Therefore, we cannot rule out the contribution of gene silencing in Kupffer cells and hepatocytes on the anti-fibrotic outcome.

Our strategy to identify novel players in tissue fibrosis took advantage of recent transcriptomic datasets for myofibroblasts and their precursors isolated from fibrotic liver or kidney in mouse models.[6,7] Using

siRNA-LNP delivery technology, we tested the effect of gene silencing in a physiologically relevant context in vivo. We employed a CCl_4 administration model that featured significant collagen accumulation and established several robust RNA and histological measures of fibrogenic activity to identify fibrosis modifiers. Using the criteria of significant reduction of *Col1a1* mRNA levels, we identified seven modifiers of interest out of 24 tested genes. Of greatest interest are those that also reduced collagen accumulation in the tissue, namely, *Egr2*, *Atp1a2*, *Fkbp10*, *Fstl1*, and *Has2*. Notably, these five genes were the most strongly silenced in vivo (by 75% or greater) that significantly reduced *Col1a1* mRNA levels. It is possible that we might have achieved a greater degree of in vivo gene silencing for other target genes with a higher dose or a different dosing paradigm. Thus, although we cannot draw conclusions about the functional role of genes whose silencing was incomplete, our results clearly identify five genes as novel fibrogenic mediators in liver fibrosis in vivo. These
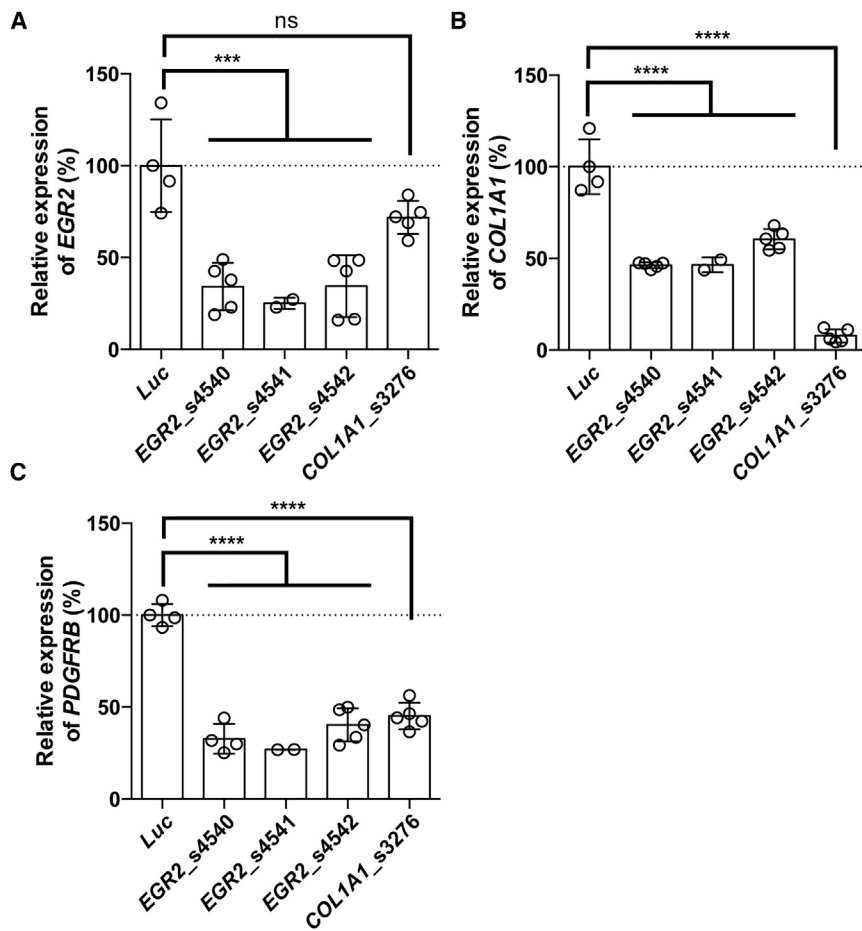
Figure 4. KD of *EGR2* Reduces *COL1A1* and *PDGFRB* mRNA Levels in Human HSC Line

(A–C) Graphs show the effect of siRNA-KD of the indicated genes (x axis) on relative mRNA levels of *EGR2* (A), *COL1A1* (B), and *PDGFRB* (C). The effect of three independent siRNAs against *EGR2* is shown. Data are presented as mean ± SD. Statistical comparisons were performed using one-way ANOVA and Dunnett's post test. Statistical differences are indicated as ***$p < 0.001$ and ****$p < 0.0001$. ns, not significant.

genes fell into different groups based on the effects of their silencing on a mini mRNA array and histological measures. We propose grouping them as follows: *Egr2*, a gene with potential function in HSC expansion; *Atp1a2* and *Fkbp10*, genes that regulate mechanosensing; and *Fstl1* and *Has2*, genes involved in matrix-cell signaling.

Egr2, a TF of the EGR family, emerged as the strongest effector in the siRNA screen. EGR TFs are important for the induction of cellular programs, including cell proliferation, differentiation, and death, in response to stimuli such as cytokines, growth factors, and toxic substances.[17–19] *Egr2* has not been previously reported to play a role in tissue fibrosis in vivo.[20] Rather, EGR2 is prominently known for its role in early myelination of the peripheral nervous system in humans and mice.[21–23]

Egr2 KD silenced its expression by 94%, reduced *Col1a1* and *Col3a1* mRNA levels, and diminished accumulation of myofibroblasts and macrophages, each to 15% of control. Liver fibrosis was also alleviated because collagen accumulation was reduced by half. Thus, our demonstration of reduced fibrogenic activity by *Egr2* silencing reveals a novel EGR2 function. The downregulation of *Pdgfrb* mRNA levels by 45% suggests that EGR2 may promote HSC expansion. This mechanism would explain the reduced aSMA-expressing HSC and thereby reduced signals for macrophage accumulation, all of which may have contributed to the reduction in fibrosis. Importantly, we also directly demonstrate that *EGR2* KD in a human HSC line reduces *COL1A1* and *PDGFRB* transcripts, supporting the regulation of a fibrogenic program in HSCs by this TF. The comparatively weaker effect of *COL1A1* silencing in vitro (∼50%) versus in vivo siRNA-LNP- mediated KD (80%) of *EGR2* is due to the use of different delivery methods as well as the use of different siRNA sequences to achieve gene silencing in human cells versus in vivo in mice. Interestingly, *COL1A1* KD also reduced *PDGFRB* mRNA levels. Because ECM accumulation and expression of PDGFRβ are linked,[24] it is feasible that decreased collagen production would decrease PDGFRβ expression in a feedback loop. The relevance of our finding to fibrogenesis in humans is also supported by a prior in vitro study, in which overexpression of *Egr2* in human skin fibroblasts upregulated collagen gene expression and myofibroblast differentiation, and these profibrotic TGF-β-induced responses were attenuated by *Egr2*-depletion.[25]

Egr2 targeting in our in vivo assay platform revealed interesting results. We unambiguously confirmed that our siRNA is specific for *Egr2* (Figures S4A–S4C) and also found that *Egr2* KD in human HSCs reduces *COL1A1* and *EGR2*, but not *EGR1* or *EGR3* mRNA (data not shown), confirming the anti-fibrotic effect. However, in vivo *Egr2* KD also decreased the mRNA levels of *Egr1* and *Egr3*, supporting the co-regulation of these transcription factors. It has been shown previously in vitro that overexpression of *Egr1* induced *Egr2* and *Egr3* expression and likewise *Egr3* overexpression induced *Egr1* and *Egr2* expression, whereas overexpression of *Egr2* did not have such an effect.[25–27] Here, we report that *Egr2* KD also reduces *Egr1* and *Egr3* mRNA levels in vivo, a novel aspect of EGR TF co-regulation. Although *Egr2* has not been previously reported to play a role in tissue fibrosis in vivo,[20] *Egr1* and *Egr3* have been implicated in the fibrotic response in vitro and in vivo previously.[27–29] Therefore, the extent of the anti-fibrotic effect may be due the co-regulation of EGR TF.

Atp1a2 and *Fkbp10* were identified as fibrogenic modulators, with mechanisms of action distinct from that of *Egr2*. ATP1A2 is the large catalytic subunit of an enzyme that catalyzes the hydrolysis of ATP, coupled with the exchange of Na^+ and K^+ ions across the plasma membrane. ATP1A2 has a known function in the contractility of skeletal and cardiac muscle.[30] On the basis of our results, it is intriguing to speculate that *Atp1a2* silencing may have reduced the contractility of myofibroblasts, effectively mimicking their behavior in a more compliant matrix environment and hence resulting in a less fibrogenic program.[31,32] Supporting this theory, we found that *Atp1a2* KD reduced fibrogenesis in vivo by significantly limiting the transcription of the *Col1a1* and *Timp1* genes, macrophage accumulation, and collagen deposition. However, in contrast to *Egr2*, *Atp1a2* silencing had no effect on aSMA expression. This pattern suggests that the myofibroblasts are generated but have reduced mechanosensing function. This theme of altered mechanosensing may also explain the alleviated fibrosis upon silencing of *Fkbp10*. FKBP10 is a molecular chaperone in the endoplasmatic reticulum that directly interacts with collagen I, contributing to the maturation and molecular stability of type I procollagen, promoting normal secretion, stable inter-molecular crosslinking, and collagen deposition in the ECM.[33] FKBP10 has a well-established role in bone mass in humans and mice, but its role in tissue fibrosis is largely unexplored.[34] *Fkbp10*$^{-/-}$ mouse embryos are post-natally lethal and display reduced collagen crosslinking in calvarial bones.[35] In this study, we report our novel finding that *Fkbp10* silencing reduces collagen deposition to 64%; however, we found no reduction in aSMA expression. We speculate that *Fkbp10* silencing alters the quantity or crosslinking of the ECM and thereby alters mechanosensing. Consistent with our in vivo results, a prior in vitro study showed that inhibition of FKBP10 in primary human fibroblasts from pulmonary fibrosis patients attenuates expression of pro-fibrotic genes and decreases collagen secretion.[36] Thus, our findings expand the scope of *Atp1a2* and *Fkbp10* functions by demonstrating their novel roles in fibrogenesis in vivo.

Fstl1 and *Has2* silencing also affected multiple fibrogenic readouts in our assay platform, but resulted in a pattern distinct from that of *Egr2*, *Atp1a2*, and *Fkbp10*. Both *Fstl1* and *Has2* silencing reduced *Col1a1* mRNA, macrophage accumulation, and collagen deposition but counterintuitively increased myofibroblast density as well as the level of *Timp1* mRNA, a profibrotic pathway. FSTL1 is a TGF-β-inducible, secreted, matricellular glycoprotein belonging to the secreted protein acidic rich in cysteines (SPARC) family, with pleiotropic functions.[37–39] During the course of our current study, it was reported that haplodepletion of *Fstl1* or a neutralizing anti-FSTL1 antibody reduced bleomycin-induced pulmonary fibrosis.[38] We found that *Fstl1* gene silencing reduced collagen transcription and accumulation in the context of liver fibrosis but surprisingly increased myofibroblast density, possibly reflecting a compensatory feedback loop. We hypothesize that the overall reduction in collagen accumulation is a direct result of decreased collagen production by *Fstl1* silencing, so that the increased number of myofibroblasts and reduced activity of collagen degradation would still result in decreased overall collagen accumulation. Indeed, KD of *FSTL1* in

the human HSC line LX-2 resulted in decreased levels of *COL1A1* mRNA.

Like *Fstl1*, silencing of *Has2* resulted in unexpected effects, also likely through a matrix-modifying mechanism. HAS2 is one of three isoenzymes responsible for cellular hyaluronan (HA) synthesis, a matrix component normally highly abundant in joint synovium. HA is well known for its role in wound healing.[40,41] *Has2* has been previously reported to be pathological in the bleomycin-induced lung fibrosis model, in which mesenchymal cell-specific deletion of *Has2* abrogated myofibroblast accumulation and inhibited the development of lung fibrosis.[42] We show that *Has2* silencing also reduces liver fibrosis. *Has2* silencing also unexpectedly augmented myofibroblast density. Taken together, our studies have identified *Fstl1* and *Has2* as fibrosis modifiers in our in vivo liver fibrosis platform and reveal surprising effects of silencing these genes, supporting their complex role in the regulation of fibrogenesis.

To the best of our knowledge, our study is the first example of a targeted siRNA assay for the discovery of novel fibrosis modifiers in vivo. The results implicate five novel modulators of the fibrogenic process in the liver and demonstrate the feasibility of siRNA-LNP for interrogating gene function in the liver. Because these genes are commonly upregulated in pericytes and myofibroblasts in both liver and kidney fibrosis models, these genes warrant follow-up to further explore their function and mechanism of action in liver and other organs and to inform their role in both physiological and pathophysiological fibrosis.

MATERIALS AND METHODS
Animal Experiments
All animal procedures were conducted in accordance with Cambridge laws and the Institutional Animal Care and Use Committee approved protocol No. 657. 8- to 10-week-old male BALB/c mice (Taconic Bioscience) were given CCl_4 by oral gavage (Sigma-Aldrich; 1 mL/kg dissolved in mineral oil) on days 0 and 7. Mineral oil alone was used as a control. In some experiments, siRNA-LNPs were given by tail vein injection. siRNA-LNPs were either given on day 6 at a concentration of 1 mg/kg or on days −7, −3, 2, and 6 at 0.5 mg/kg. These experiments were controlled with cohorts of mice that received siRNA targeting *Luciferase* (*Luc*-LNPs) with oil or CCl_4, respectively. Animals were sacrificed on day 10 by CO_2 asphyxiation, followed by cardiac perfusion with 10 mL of PBS, and liver lobes were harvested for qPCR and histopathological analysis.

Gene Selection
Target fibrosis modifier genes were selected by intersecting transcriptomic data generated from isolated HSCs of mice treated with CCl_4 for 2 months, and genes specifically expressed in pericytes/myofibroblasts in the mouse kidney 2 and 5 days after UUO.[6,7] 169 genes were common to both datasets and significantly upregulated at least 2-fold. Among these, we excluded transcripts that were not associated with a gene product, genes with no known human homolog, and

well-known modifiers in fibrosis (validated in vivo by independent investigators), resulting in 24 genes for further evaluation.

siRNA Design and Synthesis

A set of ten siRNAs with canonical siRNA structures was defined for each target gene.[43] All siRNAs were directed against the coding sequence of their respective target mRNA and perfectly matched all known mRNA transcript variants of the target gene available in the NCBI reference sequence database (RefSeq DB, release 65, May 2014).

The siRNAs used in this study were designed to be a perfect match only to their target mRNA and to have $\gtrsim$ 2 mismatches within positions 2–18 of the 19-mer sequence to any other genes. The design as described above is sufficient to ensure specificity.[44,45] Specifically, at least four mismatches between the siRNA sequences of each of the genes of interest (*Atp1a2*, *Egr2*, *Fkbp10*, *Fstl1*, and *Has2*) and the readout genes *Col1a1*, *Col3a1*, *Tgfbr1*, *Pdgfrb*, and *Timp1*. Further, there were three mismatches between *Egr2* siRNA and *Egr1* sequence and more than four mismatches between *Egr2* siRNA and *Egr3* sequence.

The siRNA antisense strands lacked a seed region (nucleotides 2–7) identical to a seed region (nucleotides 2–7) of known mouse miRNAs (miRBase, release 20, June 2013). Additional similarity analysis showed that there were at least four mismatches between the siRNA sequences of each of the genes of interest (*Atp1a2*, *Egr2*, *Fkbp10*, *Fstl1*, and *Has2*) and the readout genes *Col1a1*, *Col3a1*, *Tgfbr1*, *Pdgfrb*, and *Timp1*. Further, there were three mismatches between *Egr2* siRNA and *Egr1* sequence and more than four mismatches between *Egr2* siRNA and *Egr3* sequence. From siRNAs fulfilling those criteria, the siRNAs for each final screening were selected for predicted activity based on analysis with proprietary algorithms (Axolabs, GmbH). In vivo grade siRNAs were synthesized by Axolabs, as described elsewhere.[46]

siRNA In Vitro Screen

Each of the ten aforementioned siRNA molecules/target gene was screened for its potency to KD gene expression in a cell-based reporter assay. For each target gene, the regions of their coding sequences targeted by the siRNAs were synthesized and inserted to the 3′ UTR of the firefly luciferase gene in pCMVluc(V) validation vector (Origene), generating an mRNA transcript that encodes both the luciferase (*Luc*) and the target gene when expressed in cells. 293T cells (ATCC) were co-transfected with the validation vector and the siRNAs of interest using Lipofectamine 2000 (Thermo Fisher Scientific) at 0.1-, 1-, and 10-nM concentrations to assess KD potency. siRNA binding to the target gene leads to degradation of the mRNA that encode both *Luc* and the target gene, resulting in reduced luciferase expression. Luciferase expression was measured 24 hr post-transfection in a functional assay using the Promega Luciferase Assay System (Promega), and luciferase signal was detected using a PerkinElmer EnVision Plate Reader (PerkinElmer). For each siRNA tested, the efficiency of KD was calculated as percent of luciferase signal compared to cells that were transfected with the validation vector for the target gene alone. The most potent siRNA for each target gene (>90% luciferase reduction at 1 nM siRNA in vitro) was then

formulated as LNPs for in vivo application. The sequences of the siRNAs that resulted in efficient KD ($\geq$75%) of their target gene in vivo are provided in Table S2.

siRNA LNP Formulation

siRNA-LNPs were synthesized by mixing together an siRNA-containing aqueous phase with a lipid-containing ethanol phase. The aqueous phase contained siRNA in 10 mM citrate buffer (pH 3). The ethanol phase contained ionizable lipid[11] C12-200 (Wuxi AppTec), 1,2-distearoyl-sn-glycero-3-phosphocholine (DSPC, Avanti Polar Lipids), cholesterol (Sigma), and 1,2-dimyristoyl-sn-glycero-3-phosphoethanolamine-N-[methoxy(polyethylene glycol)-2000] (C14 PEG 2000, Avanti) at a 50:10:38.5:1.5 molar ratio and 5:1 C12-200:siRNA weight ratio. The aqueous and ethanol phases were mixed together at a 3:1 volume ratio in a microfluidic chip device using syringe pumps as previously described[47] to a final siRNA concentration of 1 mg/mL. The resultant siRNA-LNPs were dialyzed overnight in a 20,000 molecular weight cut-off (MWCO) cassette against 1x PBS at 4°C. On average, siRNA-LNPs had a mean diameter of approximately 100–150 nm, with a polydispersity index between 0.1 and 0.2 as measured by Dynamic Light Scattering (ZetaSizer, Malvern Instruments). The siRNA encapsulation efficiency (approximately 60%) was determined using a modified Quant-iT Ribogreen Assay (Invitrogen) as previously described.[48] This siRNA delivery system can target multiple liver cell types, including hepatocytes, monocytes, tissue macrophages, dendritic cells (DCs), and myofibroblasts/pericytes.

RNA Expression Analysis

RNA was extracted from liver lobes with Trizol (Thermo Fisher Scientific), followed by on-column DNase digestion using RNeasy Mini Kits and RNase free DNase sets (both from QIAGEN). cDNA was generated using the High-Capacity cDNA Reverse Transcription Kit, and qPCR analysis was performed using pre-designed TaqMan primer probes (Table S3) on the QuantStudio 12K Flex Real-Time PCR System (all from Thermo Fisher Scientific) to determine the expression levels of siRNA target genes and a panel of readout genes. All procedures were conducted following the manufacturer's protocols. The relative expression of each gene was normalized to mouse or human glyceraldehyde 3-phosphate dehydrogenase (GAPDH) using the $2^{-\Delta\Delta CT}$ method, and the mean expression of each gene in the control group was set to 100%.

Histopathology

Livers lobes were fixed in 10% neutral buffered formalin and embedded in paraffin. 5-μm sections were stained with PSR using an automated Leica system according to standard protocols. Immunohistochemistry (IHC) was performed with the Ventana system. Anti-alpha-Smooth muscle actin (αSMA) IHC was performed with fluorescein isothiocyanate (FITC)-labeled mouse monoclonal antibody 1A4, followed by an anti-FITC antibody and periodic acid-Schiff (PAS) counterstain (Abcam). Anti-IBA-1 and anti-COL1A1 IHC was performed using rabbit polyclonal antibodies (cat. # 019-19741, Wako, and Genetex, cat. # GTX41286).

Image analysis was performed by writing custom algorithms with Visiopharm software. The IBA-1 positive area was limited to infiltrating macrophages by differentiating isolated single cells (largely Kupffer cells lining sinusoids) from larger round cells in clusters (periportal, largely infiltrating macrophages, sometimes filled with mineral). De novo interstitial aSMA was differentiated from endogenous aSMA in muscular arteries by performing a PAS counterstain and then programming the algorithm to distinguish vascular morphology for exclusion from quantification. Exclusion of muscular arteries was similarly performed on sections with anti-COL1A1 IHC.

siRNA Gene Silencing in Cell Lines

The human HSC line LX-2 (EMD Millipore) was transfected with siRNAs against *EGR2*, *COL1A1*, or *Luc* with Lipofectamine RNAiMAX reagent following the manufacturer's protocol. We used the following predesigned siRNAs (listed as siRNA ID): *EGR2*: s4540, s4541, and s4542; *COL1A1*: s3276; *Luc*: AM4629; and *FSTL1*: s22032, s22033, and s22034 (Thermo Fisher Scientific). RNA was isolated on day 2 after transfection using RNeasy kits with on-column DNase digestion (QIAGEN). cDNA synthesis and qPCR was performed as stated above.

293T cells (ATCC) were co-transfected with pCMV-Egr1, pCMV-Egr2, or pCMV-Egr3 (Origene) and either *Silencer* Select Negative Control No. 1 siRNA (Thermo Fisher Scientific) or siRNA against *Egr2* (Axolabs). RNA was isolated 24 hr after co-transfection using RNeasy plus kits (QIAGEN). cDNA synthesis and qPCR was performed as stated above.

Statistical Analysis

Datasets are presented as mean ± SD. Statistical significance was assessed by two-tailed, unpaired Student's t test for comparison of two groups or by one-way ANOVA, followed by the Dunnett's multiple comparisons test for more than two groups. Differences with adjusted P values of less than 0.05 were considered statistically significant. Non-adjusted P values were listed to convey trends (Table 1).

We used an SSMD[49] method to analyze the suitability of the mRNA readout genes in our siRNA-LNP/CCl$_4$ liver fibrosis platform (Figure S2). The SSMD method was used to calculate the median of differences divided by the standard deviation of the differences between the group treated with oil and the control siRNA targeting Luciferase (oil/*Luc*-LNP) and versus CCl$_4$/*Luc*-LNP. It represents the average fold change penalized by the variability of the fold change across animals. SSMD is a suitable method because it takes the variability between animals into account. For our study, a threshold of $\beta < -1.5$ was taken as the cut-off value for suitable readout genes.

SUPPLEMENTAL INFORMATION

Supplemental Information includes five figures and three tables and can be found with this article online at http://dx.doi.org/10.1016/j.omtn.2017.04.014.

AUTHOR CONTRIBUTIONS

E.H.V., D.G.A., V.K., J.D., and L.C.B. designed the study; E.H.V., L.C.B., A.A., T.R., and I.D.-L. conducted experiments; M.H., K.J.K., and F.F.M. generated critical reagents; E.H.V., L.C.B., and S.H. analyzed data; T.O.C., T.N., T.K., and D.B. reviewed and edited the manuscript; E.H.V. and L.C.B. wrote the manuscript.

CONFLICTS OF INTEREST

E.H.V., T.R., S.H., I.D.-L., T.O.C., and L.C.B. are employees and stockholders of Biogen. The remaining authors declare no conflicts of interest.

REFERENCES

1. Wynn, T.A. (2010). Fibrosis under arrest. Nat. Med. *16*, 523–525.

2. Hinz, B., Phan, S.H., Thannickal, V.J., Prunotto, M., Desmoulière, A., Varga, J., De Wever, O., Mareel, M., and Gabbiani, G. (2012). Recent developments in myofibroblast biology: paradigms for connective tissue remodeling. Am. J. Pathol. *180*, 1340–1355.

3. Darby, I.A., Zakuan, N., Billet, F., and Desmoulière, A. (2016). The myofibroblast, a key cell in normal and pathological tissue repair. Cell. Mol. Life Sci. *73*, 1145–1157.

4. Duffield, J.S. (2012). The elusive source of myofibroblasts: problem solved? Nat. Med. *18*, 1178–1180.

5. Puche, J.E., Lee, Y.A., Jiao, J., Aloman, C., Fiel, M.I., Muñoz, U., Kraus, T., Lee, T., Yee, H.F., Jr., and Friedman, S.L. (2013). A novel murine model to deplete hepatic stellate cells uncovers their role in amplifying liver damage in mice. Hepatology *57*, 339–350.

6. Kisseleva, T., Cong, M., Paik, Y., Scholten, D., Jiang, C., Benner, C., Iwaisako, K., Moore-Morris, T., Scott, B., Tsukamoto, H., et al. (2012). Myofibroblasts revert to an inactive phenotype during regression of liver fibrosis. Proc. Natl. Acad. Sci. USA *109*, 9448–9453.

7. Grgic, I., Krautzberger, A.M., Hofmeister, A., Lalli, M., DiRocco, D.P., Fleig, S.V., Liu, J., Duffield, J.S., McMahon, A.P., Aronow, B., et al. (2014). Translational profiles of medullary myofibroblasts during kidney fibrosis. J. Am. Soc. Nephrol. *25*, 1979–1990.

8. Dong, Y., Love, K.T., Dorkin, J.R., Sirirungruang, S., Zhang, Y., Chen, D., Bogorad, R.L., Yin, H., Chen, Y., Vegas, A.J., et al. (2014). Lipopeptide nanoparticles for potent and selective siRNA delivery in rodents and nonhuman primates. Proc. Natl. Acad. Sci. USA *111*, 3955–3960.

9. Sehgal, A.Z.M., Klebanov, B., Hinkle, G., Kuchimanchi, S., Shaikh, S., Maier, M., O'Shea, J., Speciner, L., Akinc, A., Anderson, D.G., Langer, R., Novobrantseva, T., Kotelianski, V., Bumcrot, D. (2012). http://www.alnylam.com/web/wp-content/uploads/2012/11/ALNY-AASLD-FibrosisPosterXPanel-Nov2012.pdf.

10. Jiménez Calvente, C., Sehgal, A., Popov, Y., Kim, Y.O., Zevallos, V., Sahin, U., Diken, M., and Schuppan, D. (2015). Specific hepatic delivery of procollagen α1(I) small interfering RNA in lipid-like nanoparticles resolves liver fibrosis. Hepatology *62*, 1285–1297.

11. Love, K.T., Mahon, K.P., Levins, C.G., Whitehead, K.A., Querbes, W., Dorkin, J.R., Qin, J., Cantley, W., Qin, L.L., Racie, T., et al. (2010). Lipid-like materials for low-dose, in vivo gene silencing. Proc. Natl. Acad. Sci. USA *107*, 1864–1869.

12. Dahlman, J.E., Barnes, C., Khan, O.F., Thiriot, A., Jhunjunwala, S., Shaw, T.E., Xing, Y., Sager, H.B., Sahay, G., Speciner, L., et al. (2014). In vivo endothelial siRNA delivery using polymeric nanoparticles with low molecular weight. Nat. Nanotechnol. *9*, 648–655.

13. Novobrantseva, T.I., Borodovsky, A., Wong, J., Klebanov, B., Zafari, M., Yucius, K., Querbes, W., Ge, P., Ruda, V.M., Milstein, S., et al. (2012). Systemic RNAi-mediated

gene silencing in nonhuman primate and rodent myeloid cells. Mol. Ther. Nucleic Acids 1, e4.

14. Calvente, C.J., Kim, Y.O., Segal, A., Kotelianski, V., Novobrantseva, T., and Schuppan, D. (2012). In vivo efficacy of C12-200 lipid-like siRNA carriers to inhibit hepatic fibrosis. Gastroenterology 142, S-942.

15. Lua, I., Li, Y., Zagory, J.A., Wang, K.S., French, S.W., Sévigny, J., and Asahina, K. (2016). Characterization of hepatic stellate cells, portal fibroblasts, and mesothelial cells in normal and fibrotic livers. J. Hepatol. 64, 1137–1146.

16. Akamatsu, T., Arai, Y., Kosugi, I., Kawasaki, H., Meguro, S., Sakao, M., Shibata, K., Suda, T., Chida, K., and Iwashita, T. (2013). Direct isolation of myofibroblasts and fibroblasts from bleomycin-injured lungs reveals their functional similarities and differences. Fibrogenesis Tissue Repair 6, 15.

17. Collins, S., Wolfraim, L.A., Drake, C.G., Horton, M.R., and Powell, J.D. (2006). Cutting edge: TCR-induced NAB2 enhances T cell function by coactivating IL-2 transcription. J. Immunol. 177, 8301–8305.

18. Skerka, C., Decker, E.L., and Zipfel, P.F. (1997). Coordinate expression and distinct DNA-binding characteristics of the four EGR-zinc finger proteins in Jurkat T lymphocytes. Immunobiology 198, 179–191.

19. Collins, S., Lutz, M.A., Zarek, P.E., Anders, R.A., Kersh, G.J., and Powell, J.D. (2008). Opposing regulation of T cell function by Egr-1/NAB2 and Egr-2/Egr-3. Eur. J. Immunol. 38, 528–536.

20. Wu, M., Melichian, D.S., de la Garza, M., Gruner, K., Bhattacharyya, S., Barr, L., Nair, A., Shahrara, S., Sporn, P.H., Mustoe, T.A., et al. (2009). Essential roles for early growth response transcription factor Egr-1 in tissue fibrosis and wound healing. Am. J. Pathol. 175, 1041–1055.

21. Bhattacharyya, S., Fang, F., Tourtellotte, W., and Varga, J. (2013). Egr-1: new conductor for the tissue repair orchestra directs harmony (regeneration) or cacophony (fibrosis). J. Pathol. 229, 286–297.

22. Beckmann, A.M., and Wilce, P.A. (1997). Egr transcription factors in the nervous system. Neurochem. Int. 31, 477–510.

23. Topilko, P., Schneider-Maunoury, S., Levi, G., Baron-Van Evercooren, A., Chennoufi, A.B., Seitanidou, T., Babinet, C., and Charnay, P. (1994). Krox-20 controls myelination in the peripheral nervous system. Nature 371, 796–799.

24. Hewitt, K.J., Shamis, Y., Knight, E., Smith, A., Maione, A., Alt-Holland, A., Sheridan, S.D., Haggarty, S.J., and Garlick, J.A. (2012). PDGFRβ expression and function in fibroblasts derived from pluripotent cells is linked to DNA demethylation. J. Cell Sci. 125, 2276–2287.

25. Fang, F., Ooka, K., Bhattacharyya, S., Wei, J., Wu, M., Du, P., Lin, S., Del Galdo, F., Feghali-Bostwick, C.A., and Varga, J. (2011). The early growth response gene Egr2 (Alias Krox20) is a novel transcriptional target of transforming growth factor-β that is up-regulated in systemic sclerosis and mediates profibrotic responses. Am. J. Pathol. 178, 2077–2090.

26. Kumbrink, J., Kirsch, K.H., and Johnson, J.P. (2010). EGR1, EGR2, and EGR3 activate the expression of their coregulator NAB2 establishing a negative feedback loop in cells of neuroectodermal and epithelial origin. J. Cell. Biochem. 111, 207–217.

27. Fang, F., Shangguan, A.J., Kelly, K., Wei, J., Gruner, K., Ye, B., Wang, W., Bhattacharyya, S., Hinchcliff, M.E., Tourtellotte, W.G., et al. (2013). Early growth response 3 (Egr-3) is induced by transforming growth factor-β and regulates fibrogenic responses. Am. J. Pathol. 183, 1197–1208.

28. Lee, C.G., Cho, S.J., Kang, M.J., Chapoval, S.P., Lee, P.J., Noble, P.W., Yehualaeshet, T., Lu, B., Flavell, R.A., Milbrandt, J., et al. (2004). Early growth response gene 1-mediated apoptosis is essential for transforming growth factor beta1-induced pulmonary fibrosis. J. Exp. Med. 200, 377–389.

29. Chen, S.J., Ning, H., Ishida, W., Sodin-Semrl, S., Takagawa, S., Mori, Y., and Varga, J. (2006). The early-immediate gene EGR-1 is induced by transforming growth factor-beta and mediates stimulation of collagen gene expression. J. Biol. Chem. 281, 21183–21197.

30. Doganli, C., Kjaer-Sorensen, K., Knoeckel, C., Beck, H.C., Nyengaard, J.R., Honoré, B., Nissen, P., Ribera, A., Oxvig, C., and Lykke-Hartmann, K. (2012). The α2Na+/K+-ATPase is critical for skeletal and heart muscle function in zebrafish. J. Cell Sci. 125, 6166–6175.

31. Wick, G., Grundtman, C., Mayerl, C., Wimpissinger, T.F., Feichtinger, J., Zelger, B., Sgonc, R., and Wolfram, D. (2013). The immunology of fibrosis. Annu. Rev. Immunol. 31, 107–135.

32. Stockbridge, L.L., and French, A.S. (1988). Stretch-activated cation channels in human fibroblasts. Biophys. J. 54, 187–190.

33. Ishikawa, Y., Vranka, J., Wirz, J., Nagata, K., and Bächinger, H.P. (2008). The rough endoplasmic reticulum-resident FK506-binding protein FKBP65 is a molecular chaperone that interacts with collagens. J. Biol. Chem. 283, 31584–31590.

34. van Dijk, F.S., Byers, P.H., Dalgleish, R., Malfait, F., Maugeri, A., Rohrbach, M., Symoens, S., Sistermans, E.A., and Pals, G. (2012). EMQN best practice guidelines for the laboratory diagnosis of osteogenesis imperfecta. Eur. J. Hum. Genet. 20, 11–19.

35. Lietman, C.D., Rajagopal, A., Homan, E.P., Munivez, E., Jiang, M.M., Bertin, T.K., Chen, Y., Hicks, J., Weis, M., Eyre, D., et al. (2014). Connective tissue alterations in Fkbp10-/- mice. Hum. Mol. Genet. 23, 4822–4831.

36. Staab-Weijnitz, C.A., Fernandez, I.E., Knüppel, L., Maul, J., Heinzelmann, K., Juan-Guardela, B.M., Hennen, E., Preissler, G., Winter, H., Neurohr, C., et al. (2015). FK506-binding protein 10, a potential novel drug target for idiopathic pulmonary fibrosis. Am. J. Respir. Crit. Care Med. 192, 455–467.

37. Chaly, Y., Hostager, B., Smith, S., and Hirsch, R. (2014). Follistatin-like protein 1 and its role in inflammation and inflammatory diseases. Immunol. Res. 59, 266–272.

38. Dong, Y., Geng, Y., Li, L., Li, X., Yan, X., Fang, Y., Li, X., Dong, S., Liu, X., Li, X., et al. (2015). Blocking follistatin-like 1 attenuates bleomycin-induced pulmonary fibrosis in mice. J. Exp. Med. 212, 235–252.

39. Murakami, K., Tanaka, M., Usui, T., Kawabata, D., Shiomi, A., Iguchi-Hashimoto, M., Shimizu, M., Yukawa, N., Yoshifuji, H., Nojima, T., et al. (2012). Follistatin-related protein/follistatin-like 1 evokes an innate immune response via CD14 and toll-like receptor 4. FEBS Lett. 586, 319–324.

40. Toole, B.P. (2004). Hyaluronan: from extracellular glue to pericellular cue. Nat. Rev. Cancer 4, 528–539.

41. Aya, K.L., and Stern, R. (2014). Hyaluronan in wound healing: rediscovering a major player. Wound Repair Regen. 22, 579–593.

42. Li, Y., Jiang, D., Liang, J., Meltzer, E.B., Gray, A., Miura, R., Wogensen, L., Yamaguchi, Y., and Noble, P.W. (2011). Severe lung fibrosis requires an invasive fibroblast phenotype regulated by hyaluronan and CD44. J. Exp. Med. 208, 1459–1471.

43. Elbashir, S.M., Harborth, J., Lendeckel, W., Yalcin, A., Weber, K., and Tuschl, T. (2001). Duplexes of 21-nucleotide RNAs mediate RNA interference in cultured mammalian cells. Nature 411, 494–498.

44. Elbashir, S.M., Martinez, J., Patkaniowska, A., Lendeckel, W., and Tuschl, T. (2001). Functional anatomy of siRNAs for mediating efficient RNAi in Drosophila melanogaster embryo lysate. EMBO J. 20, 6877–6888.

45. Miller, V.M., Xia, H., Marrs, G.L., Gouvion, C.M., Lee, G., Davidson, B.L., and Paulson, H.L. (2003). Allele-specific silencing of dominant disease genes. Proc. Natl. Acad. Sci. USA 100, 7195–7200.

46. Frank-Kamenetsky, M., Grefhorst, A., Anderson, N.N., Racie, T.S., Bramlage, B., Akinc, A., Butler, D., Charisse, K., Dorkin, R., Fan, Y., et al. (2008). Therapeutic RNAi targeting PCSK9 acutely lowers plasma cholesterol in rodents and LDL cholesterol in nonhuman primates. Proc. Natl. Acad. Sci. USA 105, 11915–11920.

47. Chen, D., Love, K.T., Chen, Y., Eltoukhy, A.A., Kastrup, C., Sahay, G., Jeon, A., Dong, Y., Whitehead, K.A., and Anderson, D.G. (2012). Rapid discovery of potent siRNA-containing lipid nanoparticles enabled by controlled microfluidic formulation. J. Am. Chem. Soc. 134, 6948–6951.

48. Heyes, J., Palmer, L., Bremner, K., and MacLachlan, I. (2005). Cationic lipid saturation influences intracellular delivery of encapsulated nucleic acids. J. Control. Release 107, 276–287.

49. Zhang, X.D., Ferrer, M., Espeseth, A.S., Marine, S.D., Stec, E.M., Crackower, M.A., Holder, D.J., Heyse, J.F., and Strulovici, B. (2007). The use of strictly standardized mean difference for hit selection in primary RNA interference high-throughput screening experiments. J. Biomol. Screen. 12, 497–509.